# Silencing SHMT2 Inhibits the Progression of Oral Squamous Cell Carcinoma Through Cell Cycle Regulation

**Yan Liao**
Sun Yat-Sen University Affiliated Stomatological Hospital https://orcid.org/0000-0002-6113-1675
**Fang Wang**
Sun Yat-sen University Affiliated Stomatology Hospital
**Yadong Zhang**
Sun Yat-Sen University Affiliated Stomatology Hospital
**Hongshi Cai**
Sun Yat-Sen University Affiliated Stomatology Hospital
**Fan Song**
Sun Yat-Sen University Affiliated Stomatology Hospital
**Jinsong Hou** (houjs@mail.sysu.edu.cn)
Department of Oral and maxillofacial Surgery, Hospital of Stomatology, Guanghua school of Stomatology https://orcid.org/0000-0001-5330-9528

**Primary research**

**Keywords:** SHMT2, oral squamous cell carcinoma, survival analysis, cell cycle, weighted gene co-expression network analysis, gene set enrichment analysis

**Posted Date:** October 7th, 2020

**DOI:** https://doi.org/10.21203/rs.3.rs-84424/v1



**Version of Record:** A version of this preprint was published at Cancer Cell International on April 16th, 2021. See the published version at https://doi.org/10.1186/s12935-021-01880-5.

# Abstract

**Background** Serine hydroxymethyltransferase 2 (SHMT2) is a vital metabolic enzyme, which catalyzes the conversion of serine to glycine in one-carbon metabolism. SHMT2 has been reported to play a crucial role in the progression of tumors, but its function in oral squamous cell carcinoma (OSCC) remains unclear.

**Method** SHMT2 expression was analyzed using publicly-available online databases, and assessed using immunohistochemistry staining of collected clinical specimens. The correlation between SHMT2 expression and the cell cycle was predicted through bioinformatic analysis, including weighted gene co-expression network analysis and gene set enrichment analysis. After transfection with siRNA CCK8 assay, Edu staining, flow cytometry, transwell, and wound healing experiments were performed to verify the functional role of SHMT2 in vitro. A stable cell line with SHMT2 silencing was established to detect the oncogenic function of SHMT2 in vivo.

**Results** We found that SHMT2 was up-regulated in OSCC tissues and cell lines, and high level of SHMT2 was significantly linked with a poorer clinical outcome for OSCC patients. Bioinformatic analysis found that SHMT2 was closely related with cell cycle regulation. Down-regulation of SHMT2 effectively suppressed the proliferation rate of OSCC cells, and induced the prolongation of the G1 phase of the cell cycle in vitro. Western blotting found that cell cycle-related regulators such as cyclin-dependent kinase 4 (CDK4) and cyclinD1 expression levels were increased, while the expression levels of the cyclin-dependent kinase inhibitors p21Cip1 and p27Kip1 were decreased after SHMT2 knockdown. Invasive and migrative ability and epithelial mesenchymal transition were impaired by SHMT2 knockdown. Silencing SHMT2 in the HN6 cell line using short hairpin RNA impeded tumor growth in vivo.

**Conclusion** Our findings suggested that high expression of SHMT2 in OSCC indicated low survival rates, and was associated with malignant behaviors of OSCC. SHMT2 may serve as a novel prognostic and therapeutic target of interest in OSCC.


# Introduction

Oral squamous cell carcinoma (OSCC) is the most common malignant tumor in head and neck region, accounting for more than 90% of oral cancers [1]. Many risk factors are responsible for the high incidence of OSCC, such as smoking, drinking alcohol, and chewing betel quid [2]. Despite advances in diagnosis and treatment, OSCC is the leading cause of morbidity and mortality in oral cancer patients, and the five-year survival rate remains unsatisfactory, at approximately 58.7% in Asia [3, 4]. The high recurrence and lymph node metastasis rate of patients with the condition, even after treatment, are the most difficult problems facing oral clinicians at present [5, 6]. It is therefore necessary to clarify the molecular mechanisms underlying OSCC and to find a novel tumor biomarker for the diagnosis of early-stage OSCC, in order to provide timely treatment and improve the survival rate of patients.

Tumor cells undergo active metabolism during the cell cycle to support the rapid synthesis of metabolites [7]. In order to meet the energy requirements of rapid cell proliferation, tumor cells reprogram their metabolism to produce ATP through glycolysis rather than through oxidative phosphorylation, a phenomenon which is known as the Warburg effect [8-10].The Warburg effect involves a series of metabolic alterations in tumors, including aerobic glycolysis, abnormally high glucose uptake and one-carbon metabolism [11]. One-carbon metabolism plays a pivotal role in these metabolic adaptions, providing essential precursors for the synthesis of protein, nucleotides and lipids, and methyl groups for the production of DNA [12]., Mitochondrial serine hydroxylmethyltransferase2 (SHMT2) has been found to be a central enzyme in one-carbon metabolism [11].

SHMT2, located on human chromosome 17, is responsible for encoding the mitochondrial form of a pyridoxal phosphate-dependent enzyme [13]. An important paralog of SHMT is SHMT1, which is mainly present in the cytoplasm [14]. SHMT2 is primarily involved in catalyzing the conversion of serine to glycine, and simultaneously transfers b-carbon from serine to hydrolyzed tetrahydroflate (THF) to form 5,10-methylenettrahydrofolate (Me THF)[13, 15]. As the hub of serine catabolism and single carbon metabolism, SHMT2 plays a regulatory role, in which small molecular metabolites control cell proliferation [16]. SHMT2 has been reported to be up-regulated in a variety of cancer types such as breast cancer, hepatocellular carcinoma, and lung cancer, and elevated SHMT2 is significantly associated with poor prognosis of patients [17-19]. In glioma cells, SHMT2 has been shown to contribute to cell proliferation in ischemic and hypoxia tumor microenvironments [20]. SHMT2 appears to play an essential part in the progression of solid tumors, which encouraged us to explore the role of SHMT2 in OSCC.

In this study, we focused on the potential role of SHMT2 in OSCC malignant progression. We investigated the expression of SHMT2 and the relationship between its level of expression and the clinicopathological characteristics of the patients. We analyzed the pathways related to SHMT2 using bioinformatics, and verified the function of SHMT2 with experiments *in vitro* and *in vivo*. Our findings suggested that the inhibition of SHMT2 blocked cell proliferation in the G1 phase by affecting the expression of cell cycle regulators, leading to cell growth stagnation.

# Materials And Methods

### Patients and tissue samples

At the Hospital of Stomatology, Sun Yat-Sen University, we collected 91 oral squamous cell carcinoma tissue samples and 10 adjacent non-tumor tissue samples between September 2016 and January 2020. The cancer patients were selected based on their clinical and pathological information. Patients who had undergone preoperative radiotherapy or chemotherapy were excluded. We took two identical tissue samples from each patient. One was stored at -80°C for RNA extraction, and the other was fixed in formalin and embedded in paraffin for immunohistochemical analysis. All patients signed informed consent forms, and the study was approved and supervised by the Institutional Research Ethics Committee of the Hospital of Stomatology, Sun Yat-Sen University.

## Cell lines, Cell Culture, and Transfection

The human OSCC cell lines HN6, HSC3, CAL33, SCC15, and SCC25 were purchased from The America Type Culture Collection. HSC3 and CAL33 cells were cultured in Dulbecco's modified Eagle's Serum (DMEM, Gibco, USA) supplemented with 10% fetal bovine serum (FBS, Gibco, USA). HN6, SCC15, and SCC25 cells were grown in DMEM/Hams F12 medium (DMEM/F12, Gibco, USA) containing 10% FBS. NOK cells were grown in keratinocyte SFM medium mixed with growth factor. All cells were cultured at 37℃ in a humidified incubator with 5% $CO_2$.

RNA interference and transfection were conducted to test the function of SHMT2 in OSCC. The short-interfering RNA was synthesized by Ruibo Biotechnology Co., Ltd. (Guangzhou, China). The sequences specific to SHMT2 were:

si-SHMT2-1: 5'-GTGATTCCCTCGCCTTTCA-3'

si-SHMT2-2: 5'-AGACCGAAGTGCCATCACA-3'

si-SHMT2-3: 5'-CGAGGCTACTCACTGGTAT-3'

HN6 and HSC3 cells were cultured in six-well plates. After the cell density reached 80%, the cells were washed twice with PBS. The transfection reagent was then prepared. For mixture one, 5 μl lipofectamine RNAi-MAX Transfection Reagent (Invitrogen; Thermo Fisher Scientific Inc.) was added to 125 μl Opti-MEM (Invitrogen; Thermo Fisher Scientific Inc.) medium according to the manufacturer's instructions. For mixture two, 5 μl siRNA was diluted with 125 μl Opti-MEM. Mixture one and mixture two were mixed in one tube and incubated for 10 min at room temperature. After incubation, cells were grown with 250 μl of the mixture and 750 μl complete medium at 37℃ with 5% $CO_2$ for 12 h. Then 1 ml of complete medium was introduced into the transfection medium. Cells were collected 48 h after transfection for subsequent experiments.

## Immunohistochemistry

Immunohistochemistry (IHC) was performed as follows. The paraffin-embedded tissues were cut into 4.0 mm sections for dewaxing and dehydration. Staining was carried out using antigenic retrieval and goat serum block (AR0009, Boster Bio, Wuhan, China). The sections were incubated with primary antibody against SHMT2 (1:500, GeneTex), Ki-67 (1:200, ab16667, Abcam), $p21^{Cip1}$ (1:50, 12D1, Cell Signaling), $p27^{Kip1}$ (1:50, ab32034, Abcam), and CyclinD1 (1:50, E3P5S, Cell Signaling), CDK4 (1:500, D9G3E, Cell Signaling) at the recommended dilution overnight at 4℃. Staining was then developed using diaminobenzidime (DAB, GK600510, Gene Tech, China), and the cell nuclei were stained with hematoxylin (D006, Nanjing, Jiancheng, Biotech, China). The staining score was evaluated by multiplying the staining intensity and the percentage of positive cells. The intensity of staining was scored as 0 = negative, 1 = weakly positive, 2 = positive, 3 = strongly positive. The percentage of positive cells were defined as 0% = 0; <10% = 1; ³10 to <50% = 2; ³50% to <75% = 3; ³75% = 4. The total IHC scores ranged from 0–12 and

tissues with a score ³6 were assigned to the high expression group, while those with scores <6 were placed in the low expression group.

### Western blot analysis

Cells were lysed in RIPA buffer (CW2333S, CWBIO, China) supplemented with protease inhibitor cocktail set 1 (539131, Millipore, USA) and phosphatase inhibitor. Protein concentrations were measured using BCA protein assay kits (CW0014S, CWBIO). Equal amounts of total cell lysate were separated using 10% SDS-PAEG (P0014B, CWBIO) and transferred to PVDF membranes (ISEQ00010, Millipore, USA) blocked with 5% bovine serum albumin (0332, Ameresco) for 1 h at room temperature. Then the blots were incubated with the primary antibodies against SHMT2 (1:1,000, GeneTex), E-cadherin (1:1,000, 24E10, Cell Signaling), ZO1 (1:1000, D7D12, Cell Signaling), N-cadherin (1:1,000, D4R1H, Cell Signaling), Vimentin (1:1,000,D21H3,Cell Signaling b-catenin (1:1,000, D10A8, Cell Signaling), $p21^{Cip1}$ (1:1000, 12D1, Cell Signaling), $p27^{Kip1}$ (1:1000, D69C12, Cell Signaling), Cyclin D1(1:1000, E3P5S, Cell Signaling), CDK4(1:1000, D9G3E, Cell Signaling), b-actin (1:1000,13E5, Cell Signaling), and GAPAH (1:1,000,D16H11, Cell Signaling) at 4°C overnight. Membranes were incubated in HRP-conjugated secondary antibody (1:2000, 7074S, Cell Signaling) for 1 h at room temperature. The protein bands were exposed using a chemiluminescent substrate (WBKLS0500, Millipore, USA), and quantitatively analyzed using ImageJ[21].

### Quantitative reverse transcription polymerase chain reaction (qRT-PCR)

Total RNA was extracted from the cultured cells and tissues using RNAzol® RT (RN190, Molecular Research Center, USA) according to the manufacturer's protocol. The quality and quantity of the RNA were examined using a NanoDrop® ND-1000 Spectrophotometer (Thermal Fisher, Wilmington, DE, USA). RNA was reverse transcribed into cDNA using the PrimeScript RT reagent Kits (RR036A, Takara Bio, Japan). All samples were tested using SYBR Master Mix (11201ES208, Yeasen, China). The quantity of mRNA was calculated using method $2^{-DDCt}$ and normalized to GAPDH. The prime sequences were as follows:

SHMT2-forward: 5'-GCCACGGCTCATCATAGCTG-3'

SHMT2-reverse: 5'-AGCAGGTGTGCTTTGACTTCA-3'

P21-forward: 5'-GTCCACTGGGCCGAAGAG-3'

P21-reverse: 5'-TGCGTTCACAGGTGTTTCTG-3'

P27-forward: 5'-TTCATCAAGCAGTGATGTATCTGA-3'

P27-reverse: 5'-AAGAAGCCTGGCCTCAGAAG-3'

CyclinD1-forward: 5'-AACTACCTGGACCGCTTCCT-3'

CyclinD1-reverse: 5'-CCACTTGAGCTTGTTCACCA-3'

CDK4-forward: 5'-GTCGGCTTCAGAGTTTCCAC-3'

CDK4-reverse: 5'-TGCAGTCCACATATGCAACA-3'

GAPDH-forward: 5'-CCTTCCGTGTCCCCACT-3'

GAPDH-reverse: 5'-GCCTGCTTCACCACCTTC-3'

### CCK-8 Assay

The proliferation of OSCC cell lines was detected using cell counting Kit-8s (CCK-8, 40203ES80, Yeasen, China), at 0, 24, 48, 72, 96 h. In brief, $2 \times 10^3$(HN6) or $3 \times 10^3$ (HSC3) cells/well were seeded in 96-well culture plates, in triplicate. At the end of the experiment, 100 ml of 10% CCK-8 reagent (10 ml CCK-8 and 90 ml serum-free media) was added to each well, and the plates were incubated for 1 h at 37℃. Absorbance was measured at 450 nm using a microplate reader (Bio-Read, USA).

### Migration and invasion assays

Cell motility was evaluated by migration and invasion assays using Matrigel (10 mg/ml, 354234, Corning, China) and trans-well filters (pore size, 8μm; BD Biosciences). And for invasion assay, 0.33 mg/ml Matrigel was coated on the upper chamber of Transwell assay plates 2h in advance. While for migration assay, Matrigel was not required. Briefly, $3 \times 10^4$ HN6 cells or $4 \times 10^4$ HSC3 cells were seeded into the upper chambers with 200 μl serum-free medium, while the lower chambers were supplemented with 600 μl complete medium. After 24 hours, the cells on the upper filter were removed, while those on the lower chamber were fixed with paraformaldehyde and stained with 0.1% crystal violet. The cells in five random fields were subsequently counted under the microscope to assess the number of nuclei.

### Wound healing assay

Cell migration and repair ability were assessed using wound healing assays. OSCC cells were seeded in six-well plates and cultured to cover 90% of each well. Scratches in the cell layer were made with a 1 ml sterile pipette tip, and cells were washed twice with phosphate-buffered saline (PBS). After that, cells were cultivated with serum-free medium. Cells were photographed under a light microscope at 0 h, 24 h, and 48 h. The ImageJ software was used to quantify the distance between cell edges, and to calculate the wound healing rate.

### Flow cytometry analysis

Following centrifugation, $2 \times 10^5$–$2 \times 10^6$ cells were collected, and the supernatant removed. The cells were resuspended in PBS, centrifuged again, and the supernatant discarded. Then 1 ml DNA staining solution and 10 μl permeabilization solution (Multi Sciences) was added to each tube, and cells were

incubated at room temperature without light. Finally, cells were measured using Beckman flow cytometry and data was analyzed using FlowJo (https://www.flowjo.com/) Software.

### EDU staining

KFluor488 Click-it EdU imaging detection kits (KeyGen Biotech, Jiangsu, China) were used to assess the cell proliferation**.** Cells were grown in 24-well plates, and were incubated with 50 uM EdU for 2 h at temperature. Cells were fixed with 4% paraformaldehyde in PBS and osmosis was promoted with 0.5% Triton X-100 in PBS. Click-iT reaction mixture was prepared for EdU detection, and Hoechst 33342 was used to re-stain DNA. Finally, the cells were photographed with an inverted fluorescence microscope and counted using ImageJ software, based on the stained nuclei.

### Lentiviral Short Hairpin RNA (shRNA) Transfection

A stable knockdown of SHMT2 expression using shRNA was established, to detect the function of SHMT2 *in vivo*. The lentivirus packaging process was carried out by Cyagen US Inc. Lentivirus carrying shRNA targeting SHMT2 was used to achieve stable knockdown of SHMT2 expression. The sequence of the targeting vector was:

HN6-shSHMT2-1: 5'-CTTCGAGTCTATGCCCTATAACTCGAGTTATAGGGCATAGACTCGAAG -3'

HSC3-shSHMT2-2:

5'-CGGAGAGTTGTGGACTTTATACTCGAGTATAAAGTCCACAACTCTCCG -3'

### Tumor Xenografts

Female five-to six-week-old NOD/SCID mice were randomly divided into two groups, the sh-SHMT2 group and the control group, with eight mice in each group. Then, $2 \times 10^6$ HN6 cells suspended in 200 ml PBS were subcutaneously inoculated into the left inner thighs of mice. Transplanted tumors were observed weekly, and the tumor xenografts were harvested, photographed, and fixed for the IHC four weeks after injection. Tumor volume was calculated using the following formula: volume = $(\text{width}^2 \times \text{length})/2$. All animal experiments were approved by Sun Yat-Sen University's Animal Experiment Ethics Committee and conducted in accordance with their principles of animal welfare.

### Data collection and analysis

OSCC samples (313) and normal oral mucosal tissue samples (30) were selected from the head and neck squamous cell carcinoma datasets in the Cancer Genome Atlas (TCGA) database (https://www.cancer.gov/tcga), according to the OSCC classification criteria. Carcinomas originated from the tongue, floor of the month, buccal mucosa, hard palate, alveolar ridge, and oral cavity. Samples with complete clinical information were selected for further analysis. The 313 OSCC samples selected were divided into an SHMT2 low-level group and a high-level group, according to the median expression level

of SHMT2. The R software (http://www.R-project.org/) was used to perform survival analysis, weighted gene co-expressed network analysis (WGCNA) and gene set enrichment analysis (GSEA). The results of the bioinformatic analysis of the TCGA database were validated using GSE30784 from the Gene Expression Omnibus database (https://www.ncbi.nlm.nih.gov/).

### Weighted gene co-expressed network analysis

The top 50% genes with the highest variance were selected among 10215 genes for WGCNA analysis using the R "WGCNA" package. A gene expression similarity matrix was constructed with which to analyze the cooperative expression between genes. An adjacency matrix was built based on the above matrix, and an appropriate soft threshold was introduced to establish a scale free network. A topological overlap matrix (TOM) was constructed by defining a measure of node dissimilarity. Network modules were then identified using dynamic hierarchical tree clustering. Finally, we selected the most relevant module with which to further analyze the correlation between modules and clinical parameters in OSCC using Gene Ontology annotation (GO)[22, 23] and the Kyoto Encyclopedia of Genes and Genomes pathway (KEGG)[24] enrichment analysis.

### Gene set enrichment analysis

GSEA software (http://software.broadinstitute.org/gsea/index.jsp) was used to conduct the enrichment analysis on the groups with high expression of SHMT2 and low expression of SHMT2 to evaluate the trend of distribution of SHMT2 in the gene table of OSCC biological phenotypic relevance sequencing, and to determine its contribution to the phenotype. A *P*-value < 0.05 and a false discovery rate (FDR) <0.05 were considered as credible enrichment.

### Statistical analysis

All *in vitro* experiments were repeated at least three times. The mean and the standard deviation of data were analyzed by GraphPad Prism 8.0 software. The difference between the two groups was analyzed using two-tailed Student's t-tests, and ANOVAs were used for the multiple groups. The correlations between SHMT2 expression and the clinicopathological features of the OSCC patients were analyzed using chi-square tests or Fisher's exact tests. Survival curves were constructed using the Kaplan-Meier method and tested with log-rank. SPSS 25.0 was applied to establish a Cox proportional hazard regression model for univariate and multivariate analysis. The differences were considered statistically significant at $p < 0.05$ (* $p < 0.05$, ** $p < 0.01$, *** $p < 0.001$).

## Results

### SHMT2 is up-regulated in OSCC and is associated with poor prognosis for patients

By analyzing SHMT2 expression in published profiles from the TCGA database we found that SHMT2 was more highly expressed in 313 OSCC samples, than in 30 normal tissue samples (Figure 1a), and that expression of SHMT2 was positively related with pathologic stage (Figure 1b). To exclude individual

differences, we analyzed 30 pairs of OSCC tissues and normal tissues from the TCGA database, and obtained similar results (Figure 1c). Survival analysis showed that high expression of SHMT2 was statistically significant, with lower overall survival, disease free survival, and disease specific survival in OSCC patients (Figure 1d).

We examined our clinical samples for SHMT2 expression in OSCC. Immunohistochemistry staining analysis showed that SHMT2 was overexpressed in tumor tissues compared with adjacent tumor tissues (Figure 1d-e). Moreover, moderately and poorly differentiated tumors had higher stain scores than well differentiated tumors (Figure 1d-f). Analysis of the relationships among a series of clinicopathological features revealed that high levels of SHMT2 were significantly positively associated with age, alcohol history, pathologic tumor stage, clinical stage, histologic grade and perineural invasion (Table 1). Univariate and multivariate analysis of OSCC patients in the TCGA database demonstrated that SHMT2 could be an independent prognostic factor for poor overall survival (Table 2). To investigate SHMT2 expression in OSCC cells, we tested the mRNA and protein levels of SHMT2 in five OSCC cell lines (HN6, HSC3, CAL33, SCC15, and SCC25) and in one normal oral epithelial cell line (NOK). Both mRNA and protein expression of SHMT2 in oral cancer cells was higher than that in normal oral epithelial cells (Figure 1h-i). These results indicate that high levels of expression of SHMT2 in OSCC might be indicative of an unfavorable prognosis.

## Construction of a weighted co-expression network and identification of the key module

WGCNA is a typical systems biology algorithm for constructing gene co-expression networks, which aims to find gene network modules of cooperative expression and explore the correlation between gene networks and clinical parameters. In this study, seven abnormal cases were excluded, according to the connection filtering threshold and a total of 306 samples were clustered using WGCNA (Figure 2a). Based on a function in the WGCNA package, we chose the power of b = 5 (scale free $R^2$ = 0.84) as the soft-thresholding to satisfy the scale free topology (Figure 2b-c). The adjacency matrix was then converted into a topological matrix (TOM) by calculating the topological overlap between genes. As shown in the clustering dendrogram, 15 modules were merged, based on the height of module eigengenes higher than 0.2 (Figure 2d-e). Among these modules, the tan module ($r$ = 0.56, $p$ < 0.0001) had the closest correlation with SHMT2. The tan module was therefore chosen as the key module for subsequent analysis (Figure 2f). We also conducted WGCNA for GSE30784 to validate the results of OSCC samples in the TCGA database (Additional file 1: Figure S1).

## Go, KEGG, and GSEA analysis of the hub module

We performed GO annotation and KEGG enrichment analysis for the tan module, to explore the biological function of SHMT2, using the R package “cluster Profiler”. The results of the GO analysis indicated that the tan module was mainly involved in the biological processes of positive regulation of cell cycle and meiotic cell cycle (Figure 3a). KEGG provided similar results, with the genes being most significantly enriched in the cell cycle (Figure 3b).

GSEA was used to validate the relationship between SHMT2 expression and pathways, using the GSEA software. The terms meiotic cell cycle, positive regulation of cell cycle transition, cell cycle G1/S phase transition, cell cycle check point and cell cycle DNA replication were significantly enriched (Figure 3c-h). These results were confirmed using the GSE30784 dataset (Additional file 1: Figure S2).

## SHMT2 knockdown inhibits OSCC cell proliferation, inducing cell cycle arrest in G1 phase

Considering the pivotal role of SHMT2 in cell cycle regulation, Si-RNA specifically designed for SHMT2 was transfected into HN6 and HSC3 cell lines to verify its functional role *in vitro*. The knockdown effect was tested by PCR and western blotting, and the results indicated that the level of both mRNA and protein of SHMT2 were downregulated (Figure 4a-b). We selected two sequences with a good silencing effect, si-SHMT2-2 and si-SHMT2-3, for subsequent experiments. CCK-8 assay results demonstrated that SHMT2 knockdown suppressed the proliferation rate in HN6 and HSC3 cell lines compared with the control group (Figure 4c-d). We conducted 5-ethynyl-2'-deoxyuridine (EdU) staining to assess OSCC cell proliferation (Figure 4e). Images of EdU staining showed that SHMT2 down-regulation significantly reduced the proportion of EdU stained cells (Figure 4f). To further explore the mechanism of regulation of OSCC cell proliferation by SHMT2, we evaluated the cell cycle after siRNA treatment. Flow cytometry analysis showed that the proportion of SHMT2 knockdown cells blocked in G1 phase was significantly higher than in the control group (Figure 4g-h). We then examined changes after SHMT2 knockdown in several cell cycle regulators correlated with the G1/S transition, using RT-qPCR and western blotting. The levels of the cell cycle inhibitors $p21^{Cip1}$ and $p27^{Kip1}$ were increased by SHMT2 knockdown. Conversely, levels of the cell cycle promoters cyclinD1 and CDK4 decreased in SHMT2 silenced cells (Figure 4i-j).

## SHMT2 knockdown inhibited the invasive and migrative ability of OSCC cells

To examine the carcinogenic function of SHMT2 in OSCC, we carried out Transwell and wound healing experiments. It was found that the number of migrating and invasive cells was decreased in the si-SHMT2 treated group when compared with the corresponding control group (Figure 5a-c). The results of the wound healing experiments revealed that down-regulation of SHMT2 reduced the healing area of HN6 and HSC3 cells (Figure 5d-f). Western blotting was performed to measure epithelial mesenchymal transition-related protein level changes. We found that mesenchymal phenotype markers including N-cadherin, b-catenin, and Vimentin were downregulated, whereas epithelial phenotype markers such as E-cadherin and ZO-1 were up-regulated after SHMT2 knockdown (Figure 5g). These results indicated that SHMT2 was involved in the epithelial mesenchymal transition of OSCC.

## Silencing of SHMT2 inhibits tumor growth

To further investigate the oncogenic function of SHMT2 *in vivo*, we constructed a lentivirus knockdown-stable strain targeting SHMT2. Two different stable strain sequences, shSHMT2-1 and shSHMT2-2 were transfected into HN6 cells and HSC3 cells, respectively. Western blotting indicated that the two different sequences of shRNA significantly reduced the expression level of SHMT2 (Figure 6a-b). The results of CCK-8 assays showed that silencing SHMT2 could inhibit the growth of OSCC cells (Figure 6c-d). Then

we injected HN6 cells subcutaneously into the left inner thighs of NOD/SCID mice and observed the growth of the subsequent tumors. As can be seen in Figure 5e-g, the volumes and weights of tumors in mice in the shSHMT2 cell injection group were significantly smaller than those in mice of the control group. After sacrificing the mice, we extracted RNA from the tumors and measured the expression of the mRNA of SHMT2 and cell cycle regulators. The SHMT2 expression level was significantly reduced in tumors from the shSHMT2 mice group compared with the control group. The levels of $p21^{Cip1}$ and $p27^{Kip1}$ expression were increased, whereas cyclinD1 and CDK4 were decreased, in the shSHMT2 mice (Figure 5h). Immunohistochemistry of tumors removed from mice showed that SHMT2 and Ki-67 protein expression levels were downregulated in the shSHTM2 group (Figure 5i). P21 and P27 protein expression levels were up-regulated in the shSHMT2 group. CyclinD1 and CDK4 protein expression levels, however, were downregulated in the shSHMT2 group compared with the control group (Figure 5j). These findings support the hypothesis that SHMT2 deletion inhibited OSCC cell proliferation and tumor growth *in vivo*.

# Discussion

One-carbon metabolism provides cellular components such as nucleotides, lipids, and proteins for cell growth, and its role in tumorigenesis has attracted considerable attention in recent years [25-27]. SHMT2 is a key enzyme in one-carbon metabolism, and is responsible for the conversion of serine to glycine. Several studies have found that SHMT2 is elevated in a range of tumors, and high levels of SHMT2 are associated with poor prognosis in patients [17, 28-30]. One study found that SHMT2 contributes to cancer cell survival in the harsh tumor microenvironment, which relies on glycine clearance [20]. Another study in breast cancer demonstrated that SHMT2 acts as the first rate-limiting enzyme in one-carbon pathway, promoting rapid cell growth and increasing the potential for metastasis [31]. These findings are in accordance with our results in OSCC.

We found that SHMT2 was overexpressed in OSCC, and was associated with unfavorable clinical outcomes. Clinical significance analysis revealed that high expression of SHMT2 was significantly correlated with poor differentiation, advanced stage and perineural invasion. A further series of experiments *in vitro* and *in vivo* demonstrated that inhibition of SHMT2 impeded tumor growth and attenuated the proliferation, invasion, and migration of OSCC cells.

Uncontrolled cell cycle and dysregulated cell proliferation are the basic mechanisms leading to cancer progression [32, 33]. The cell cycle includes interphase and the division phase. Interphase is divided into three stages: the early DNA synthesis stage (G1 stage), the DNA synthesis stage (S stage) and the late DNA synthesis stage (G2 stage). During the G1 phase, the cells mainly synthesize substances other than DNA needed for mitosis, including some ribosomes and proteins. In the S phase, the cells mainly complete the synthesis and replication of DNA. In the G2 phase, cells continue to synthesize the materials needed for mitosis, such as microtubules [34]. One study has suggested that silencing the SHMT2 gene and depleting extracellular glycine prolongs the G1 phase of the cell cycle, thus slowing down the proliferation of HeLa and other cancer cells [35]. However, the molecular mechanism of SHMT2 regulating OSCC cell proliferation remains poorly understood. WGCNA and GSEA analysis, therefore, were

used to identify the gene sets related to SHMT2 expression in OSCC samples from the TCGA database. Based on the most relevant module identified by WGCNA analysis, GO, and KEGG enrichment analyses were carried out on the genes contained in the key module, and it was found that the module was primarily enriched in genes involved in the cell cycle. GSEA analysis found that the expression level of SHMT2 was positively correlated with the cell cycle, cell cycle phase transition, and cell cycle checkpoints. These findings suggest that the effect of SHMT2 on OSCC cell proliferation is primarily associated with regulation of cell cycle.

Both $p21^{Cip1}$ and $p27^{Kip1}$ are kinase inhibition proteins. The proteins they encode bind to and inhibit the activity of CDK2 or CDK4 complex, and they thus function as regulators of cell cycle progression at G1 [36-38]. Cyclin D1 belongs to the highly conserved cyclin family, and forms a complex with and acts as a regulatory subunit of CDK4, whose activity is required for the cell cycle G1/S transition [33, 34, 39, 40]. This study found that SHMT2 depletion significantly prolonged the G1 phase of OSCC cells. The cell cycle inhibitors $p21^{Cip1}$ and $p27^{Kip1}$were up-regulated, whereas the cell cycle promoters cyclin D1 and CDK4 were downregulated when SHMT2 expression was inhibited. Research in lung cancer has indicated that the cell cycle can be arrested owing to a decrease in the expression level of SHMT1 [41]. In contrast, our study suggested that silencing SHMT2 in OSCC triggered changes in cell cycle regulators and induced cell block in G1 phase of the cell cycle, resulting in a decrease in cell proliferation.

SHMT2 is responsible for the conversion of serine to glycine. Serine and glycine cooperate to provide some of the necessary metabolites for tumor cell growth [11]. Moreover, one-carbon units generated by SHMT2-catalyzed metabolic reactions facilitate the synthesis of purines [42]. Since serine/glycine metabolism is important in nucleotide biosynthesis, SHMT2 has been a target for cancer chemotherapy. Pemetrexed has been used as an antifolate drug targeting SHMT2 *in vitro* [43]. Leucovorin (N5CHO-THF) and 3-bromopyruvate (3BP) are two selective inhibitors for SHMT2 that have been examined in clinical trials [44, 45]. However, drug resistance and side effects hinder their clinical application, necessitating more work to investigate effective and specific therapeutic targets for different cancers.

Combined with bioinformatics analysis and experiments *in vivo* and *in vitro*, SHMT2 was found to be up-regulated in OSCC and actively participated in the progression of OSCC, including rapid proliferation, cell cycle arrest, enhanced invasion and cell migration. SHMT2 is therefore worthy of consideration as a new therapeutic target for OSCC.

# List Of Abbreviations

ES Enrichment score

FBS Fetal bovine serum

GO Gene Ontology

GSEA Gene set enrichment analysis

KEGG Kyoto Encyclopedia of Genes and Genomes

OSCC Oral squamous cell carcinoma

PBS Phosphate-buffered saline

TCGA The Cancer Genome Atlas

TOM Topological overlap matrix

WGCNA Weighted gene co-expressed network analysis

# Declarations


### Acknowledgements

Acknowledgements for all members involved in this study.


### Authors' contributions

JH, YZ and YL conceived and designed the experiments. YL, HC, FW performed experiments and conducted bioinformatic analysis. YL, FW, FS collected and analyzed results. YL write the original manuscript. JH and HC reviewed and edited the manuscript.


### Funding

This study was supported by National Natural Science Foundation of China [grant numbers 81874128]; Sun Yat-Sen University Clinical Research 5010 Program [grant numbers 2015018]


### Available data and materials

The datasets used in this study can be obtained from the Cancer Genome Atlas (TCGA) database (https://www.cancer.gov/tcga) and the Gene Expression Omnibus (GEO) database (https://www.ncbi.nlm.nih.gov/).

### Ethics approve and consent to participant

All patients participating in this study signed informed consent and were approved by the ethics committee of the Hospital of Stomatology, Sun Yat-Sen University. Animal experiments were supervised and approved by Sun Yat-Sen University's Animal Experiment Ethics Committee.

### Consent for publication

Not appliable

### Competing interests

The authors declare that they have no competing interests

**Author details**

[1]Department of Oral and Maxillofacial Surgery, Guanghua School of Stomatology, Hospital of Stomatology, Sun Yat-sen University, Guangzhou, Guangdong 510055, China. [2]Guangdong Provincial Key Laboratory of Stomatology, Sun Yat-Sen University, Guangzhou, Guangdong, China.

# References

1. Rezende TM, de Souza Freire M, Franco OL: **Head and neck cancer: proteomic advances and biomarker achievements**. *Cancer* 2010, **116**(21):4914-4925.
2. Gharat SA, Momin M, Bhavsar C: **Oral Squamous Cell Carcinoma: Current Treatment Strategies and Nanotechnology-Based Approaches for Prevention and Therapy**. *Crit Rev Ther Drug Carrier Syst* 2016, **33**(4):363-400.
3. Taghavi N, Yazdi I: **Prognostic factors of survival rate in oral squamous cell carcinoma: clinical, histologic, genetic and molecular concepts**. *Arch Iran Med* 2015, **18**(5):314-319.
4. Bray F, Ferlay J, Soerjomataram I, Siegel RL, Torre LA, Jemal A: **Global cancer statistics 2018: GLOBOCAN estimates of incidence and mortality worldwide for 36 cancers in 185 countries**. *CA Cancer J Clin* 2018, **68**(6):394-424.
5. Bloebaum M, Poort L, Bockmann R, Kessler P: **Survival after curative surgical treatment for primary oral squamous cell carcinoma**. *J Craniomaxillofac Surg* 2014, **42**(8):1572-1576.
6. Huang TH, Li KY, Choi WS: **Lymph node ratio as prognostic variable in oral squamous cell carcinomas: Systematic review and meta-analysis**. *Oral Oncol* 2019, **89**:133-143.
7. Vander Heiden MG, Cantley LC, Thompson CB: **Understanding the Warburg effect: the metabolic requirements of cell proliferation**. *Science* 2009, **324**(5930):1029-1033.
8. Warburg O: **On the origin of cancer cells**. *Science* 1956, **123**(3191):309-314.
9. Jones RG, Thompson CB: **Tumor suppressors and cell metabolism: a recipe for cancer growth**. *Genes Dev* 2009, **23**(5):537-548.
10. Cairns RA, Harris IS, Mak TW: **Regulation of cancer cell metabolism**. *Nat Rev Cancer* 2011, **11**(2):85-95.
11. Amelio I, Cutruzzola F, Antonov A, Agostini M, Melino G: **Serine and glycine metabolism in cancer**. *Trends Biochem Sci* 2014, **39**(4):191-198.
12. Cooling MT, Hunter P, Crampin EJ: **Modelling biological modularity with CellML**. *IET Systems Biology* 2008, **2**(2):73-79.
13. Wu M, Wanggou S, Li X, Liu Q, Xie Y: **Overexpression of mitochondrial serine hydroxyl-methyltransferase 2 is associated with poor prognosis and promotes cell proliferation and invasion in gliomas**. *Onco Targets Ther* 2017, **10**:3781-3788.

14. Anderson DD, Stover PJ: **SHMT1 and SHMT2 are functionally redundant in nuclear de novo thymidylate biosynthesis**. *PLoS One* 2009, **4**(6):e5839.
15. Wei Z, Song J, Wang G, Cui X, Zheng J, Tang Y, Chen X, Li J, Cui L, Liu CY *et al*: **Deacetylation of serine hydroxymethyl-transferase 2 by SIRT3 promotes colorectal carcinogenesis**. *Nat Commun* 2018, **9**(1):4468.
16. Yang X, Wang Z, Li X, Liu B, Liu M, Liu L, Chen S, Ren M, Wang Y, Yu M *et al*: **SHMT2 Desuccinylation by SIRT5 Drives Cancer Cell Proliferation**. *Cancer Res* 2018, **78**(2):372-386.
17. Zhang L, Chen Z, Xue D, Zhang Q, Liu X, Luh F, Hong L, Zhang H, Pan F, Liu Y *et al*: **Prognostic and therapeutic value of mitochondrial serine hydroxyl-methyltransferase 2 as a breast cancer biomarker**. *Oncol Rep* 2016, **36**(5):2489-2500.
18. Ji L, Tang Y, Pang X, Zhang Y: **Increased Expression of Serine Hydroxymethyltransferase 2 (SHMT2) is a Negative Prognostic Marker in Patients with Hepatocellular Carcinoma and is Associated with Proliferation of HepG2 Cells**. *Med Sci Monit* 2019, **25**:5823-5832.
19. Lee GY, Haverty PM, Li L, Kljavin NM, Bourgon R, Lee J, Stern H, Modrusan Z, Seshagiri S, Zhang Z *et al*: **Comparative oncogenomics identifies PSMB4 and SHMT2 as potential cancer driver genes**. *Cancer Res* 2014, **74**(11):3114-3126.
20. Kim D, Fiske BP, Birsoy K, Freinkman E, Kami K, Possemato RL, Chudnovsky Y, Pacold ME, Chen WW, Cantor JR *et al*: **SHMT2 drives glioma cell survival in ischaemia but imposes a dependence on glycine clearance**. *Nature* 2015, **520**(7547):363-367.
21. Schneider CA, Rasband WS, Eliceiri KW: **NIH Image to ImageJ: 25 years of image analysis**. *Nat Methods* 2012, **9**(7):671-675.
22. Ashburner M, Ball CA, Blake JA, Botstein D, Butler H, Cherry JM, Davis AP, Dolinski K, Dwight SS, Eppig JT *et al*: **Gene ontology: tool for the unification of biology. The Gene Ontology Consortium**. *Nat Genet* 2000, **25**(1):25-29.
23. **The Gene Ontology Resource: 20 years and still GOing strong**. *Nucleic Acids Res* 2019, **47**(D1):D330-d338.
24. Kanehisa M, Goto S: **KEGG: kyoto encyclopedia of genes and genomes**. *Nucleic Acids Res* 2000, **28**(1):27-30.
25. Newman AC, Maddocks ODK: **One-carbon metabolism in cancer**. *Br J Cancer* 2017, **116**(12):1499-1504.
26. Ducker GS, Rabinowitz JD: **One-Carbon Metabolism in Health and Disease**. *Cell Metab* 2017, **25**(1):27-42.
27. Mattaini KR, Sullivan MR, Vander Heiden MG: **The importance of serine metabolism in cancer**. *J Cell Biol* 2016, **214**(3):249-257.
28. Ning S, Ma S, Saleh AQ, Guo L, Zhao Z, Chen Y: **SHMT2 Overexpression Predicts Poor Prognosis in Intrahepatic Cholangiocarcinoma**. *Gastroenterol Res Pract* 2018, **2018**:4369253.
29. Pennisi E: **Researchers trade insight about gene swapping**. *Science* 2004, **305**:334 - 335.

30. Shi H, Fang X, Li Y, Zhang Y: **High Expression of Serine Hydroxymethyltransferase 2 Indicates Poor Prognosis of Gastric Cancer Patients**. *Med Sci Monit* 2019, **25**:7430-7438.
31. Li AM, Ducker GS, Li Y, Seoane JA, Xiao Y, Melemenidis S, Zhou Y, Liu L, Vanharanta S, Graves EE *et al*: **Metabolic Profiling Reveals a Dependency of Human Metastatic Breast Cancer on Mitochondrial Serine and One-Carbon Unit Metabolism**. *Mol Cancer Res* 2020, **18**(4):599-611.
32. Thomson PJ: **Perspectives on oral squamous cell carcinoma prevention-proliferation, position, progression and prediction**. *J Oral Pathol Med* 2018, **47**(9):803-807.
33. Mishra R: **Cell cycle-regulatory cyclins and their deregulation in oral cancer**. *Oral Oncol* 2013, **49**(6):475-481.
34. Wenzel ES, Singh ATK: **Cell-cycle Checkpoints and Aneuploidy on the Path to Cancer**. *In Vivo* 2018, **32**(1):1-5.
35. Jain M, Nilsson R, Sharma S, Madhusudhan N, Kitami T, Souza AL, Kafri R, Kirschner MW, Clish CB, Mootha VK: **Metabolite profiling identifies a key role for glycine in rapid cancer cell proliferation**. *Science* 2012, **336**(6084):1040-1044.
36. Li Y, Huang J, Zeng B, Yang D, Sun J, Yin X, Lu M, Qiu Z, Peng W, Xiang T *et al*: **PSMD2 regulates breast cancer cell proliferation and cell cycle progression by modulating p21 and p27 proteasomal degradation**. *Cancer Lett* 2018, **430**:109-122.
37. **<Resveratrol induces cell cycle arrest and apoptosis with docetaxel in prostate cancer cells via a p53 p21WAF1CIP1 and p27KIP1 pathway.pdf>**.
38. Mitrea DM, Yoon MK, Ou L, Kriwacki RW: **Disorder-function relationships for the cell cycle regulatory proteins p21 and p27**. *Biol Chem* 2012, **393**(4):259-274.
39. Li X, Seebacher NA, Garbutt C, Ma H, Gao P, Xiao T, Hornicek FJ, Duan Z: **Inhibition of cyclin-dependent kinase 4 as a potential therapeutic strategy for treatment of synovial sarcoma**. *Cell Death Dis* 2018, **9**(5):446.
40. Schafer KA: **The cell cycle: a review**. *Vet Pathol* 1998, **35**(6):461-478.
41. Paone A, Marani M, Fiascarelli A, Rinaldo S, Giardina G, Contestabile R, Paiardini A, Cutruzzola F: **SHMT1 knockdown induces apoptosis in lung cancer cells by causing uracil misincorporation**. *Cell Death Dis* 2014, **5**:e1525.
42. Martinez-Reyes I, Chandel NS: **Mitochondrial one-carbon metabolism maintains redox balance during hypoxia**. *Cancer Discov* 2014, **4**(12):1371-1373.
43. Daidone F, Florio R, Rinaldo S, Contestabile R, di Salvo ML, Cutruzzola F, Bossa F, Paiardini A: **In silico and in vitro validation of serine hydroxymethyltransferase as a chemotherapeutic target of the antifolate drug pemetrexed**. *Eur J Med Chem* 2011, **46**(5):1616-1621.
44. Chang WN, Tsai JN, Chen BH, Huang HS, Fu TF: **Serine hydroxymethyltransferase isoforms are differentially inhibited by leucovorin: characterization and comparison of recombinant zebrafish serine hydroxymethyltransferases**. *Drug Metab Dispos* 2007, **35**(11):2127-2137.

45. Paiardini A, Tramonti A, Schirch D, Guiducci G, di Salvo ML, Fiascarelli A, Giorgi A, Maras B, Cutruzzola F, Contestabile R: **Differential 3-bromopyruvate inhibition of cytosolic and mitochondrial human serine hydroxymethyltransferase isoforms, key enzymes in cancer metabolic reprogramming**. *Biochim Biophys Acta* 2016, **1864**(11):1506-1517.

# Tables

**Table1 Correlations between SHMT2 and clinicopathological characteristics of oral squamous cell carcinoma（n=103）**

| | SHMT2 expression | | |
|---|---|---|---|
| **Characteristics** | **High** | **Low** | ***p* value** |
| Age (years) | | | |
| < 61 | 25 | 30 | **0.031*** |
| ≥ 61 | 32 | 16 | |
| Gender | | | |
| Male | 39 | 32 | 0.901 |
| Female | 18 | 14 | |
| Alcohol history | | | |
| Yes | 23 | 7 | **0.005**** |
| No | 34 | 39 | |
| Tobacco smoking history | | | |
| Yes | 19 | 12 | 0.425 |
| No | 38 | 34 | |
| T stage | | | |
| T1-2 | 16 | 22 | **0.04*** |
| T3-4 | 41 | 24 | |
| N stage | | | |
| $N^-$ | 17 | 21 | 0.980 |
| $N^+$ | 40 | 25 | |
| M stage | | | |
| $M^-$ | 42 | 38 | 0.280 |
| $M^+$ | 15 | 8 | |
| Clinical stage | | | |
| I-II | 5 | 14 | **0.005**** |
| III-IV | 52 | 32 | |
| Histologic grade | | | |
| Well | 4 | 12 | **0.028*** |
| Moderately | 40 | 27 | |

| | | | |
|---|---|---|---|
| Poorly | 13 | 7 | |
| Lymph node neck dissection | | | |
| Yes | 3 | 3 | 0.554 |
| No | 54 | 43 | |
| Lymph vascular invasion | | | |
| Yes | 36 | 34 | 0.245 |
| No | 21 | 12 | |
| Perineural invasion | | | |
| Yes | 31 | 35 | **0.022*** |
| No | 26 | 11 | |
| Close or positive margin | | | |
| Yes | 34 | 35 | 0.078 |
| No | 23 | 11 | |
| Recurrence | | | |
| Yes | 35 | 36 | 0.066 |
| No | 22 | 10 | |

*represents $P < 0.05$, **represents $P<0.01$, ***represents $P<0.001$

**Table2 Univariate and multivariate analysis of various clinicopathologic characteristics related with overall survival in OSCC patients**

| | Univariate analysis | | Multivariate analysis | |
|---|---|---|---|---|
| | HR (95% CI) | *P* | HR (95% CI) | *P* |
| Gender | 1.062(0.753~1.497) | 0.733 | 0.95(0.661~1.367) | 0.783 |
| Age | 1.203(0.862~1.679) | 0.277 | 1.201(0.846~1.706) | 0.305 |
| T stage | 1.329(0.94~1.879) | 0.108 | 1.5(0.783~2.875) | 0.222 |
| N stage | 1.453(1.046~2.017) | **0.026*** | 1.51(0.991~2.299) | 0.055 |
| M stage | 0.697(0.172~2.821) | 0.613 | 0.686(0.168~2.809) | 0.601 |
| Clinical stage | 1.329(0.914~1.933) | 0.136 | 0.696(0.313~1.548) | 0.374 |
| Histological grade | 1.286(0.992~1.667) | 0.058 | 1.32(1.012~1.72) | **0.04*** |
| SHMT2 level | 1.548(1.111~2.156) | **0.01*** | 1.478(1.051~2.078) | **0.025*** |
| | | | | |

*represents $P < 0.05$, **represents $P<0.01$, ***represents $P<0.001$

# Figures

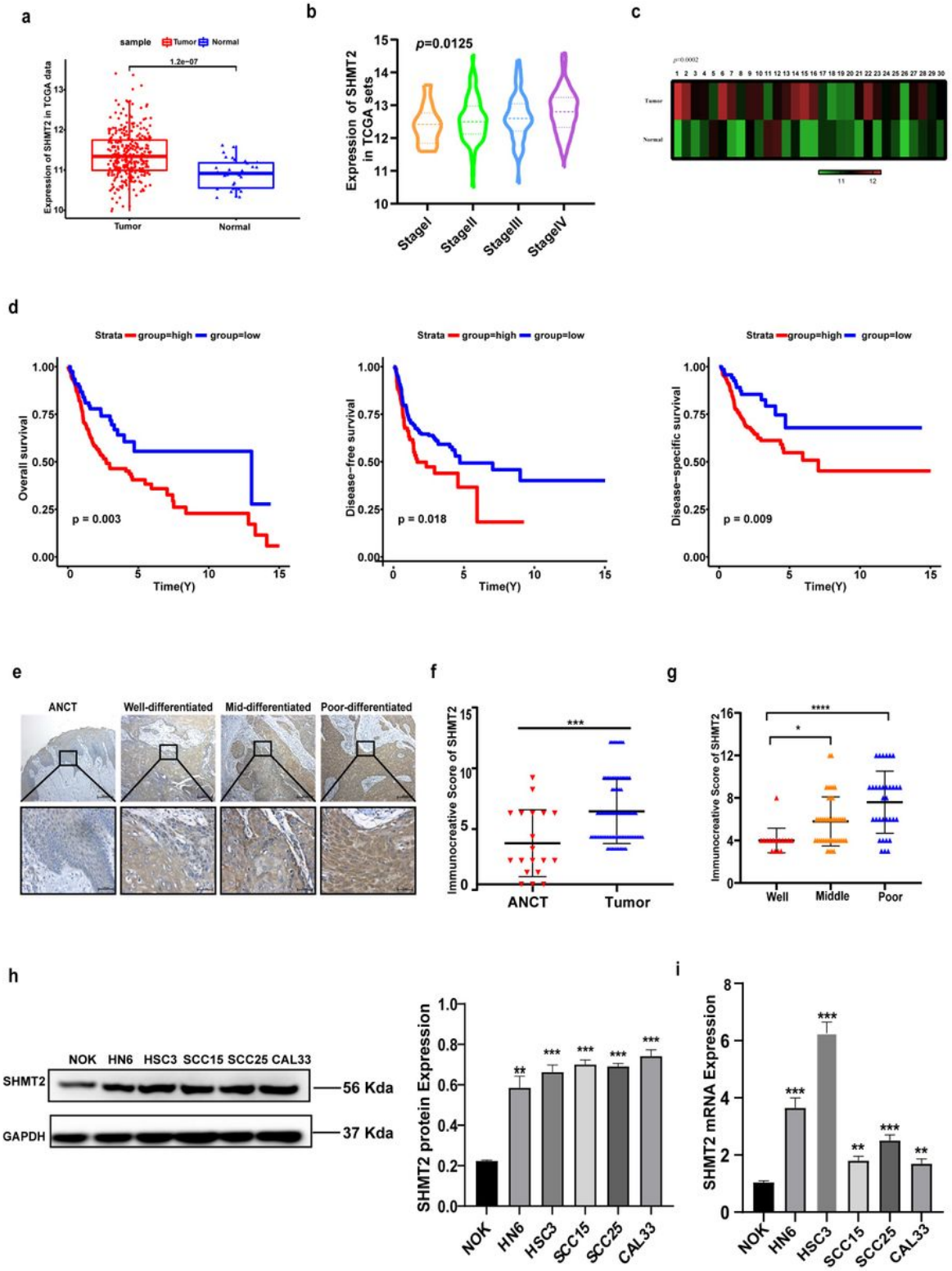


## Figure 1

SHMT2 was overexpressed in OSCC and predicted poor prognosis. (a) Relative analysis of SHMT2 mRNA in OSCC (n = 313) and adjacent normal tissues (n = 30) from the TCGA database. (b) Analysis of SHMT2 mRNA level in different stages of OSCC samples in the TCAG database (stage I, n = 11; stage II, n = 74; stage III, n = 61; stage IV, n = 149). (c) SHMT2 expression level in 30 paired oral tumor tissues and adjacent normal tissues in the TCGA database. (d) Kaplan-Meier survival curves for overall survival (n =

312), disease free survival (n = 312) and disease specific survival (n = 295) in OSCC patients with high and low expression of SHMT2. (e) Immunohistochemistry staining of SHMT2 in ANCT and tumors with different degrees of differentiation. Magnification of 100× (left) and 400× (right). (f) Immunohistochemical staining score of SHMT2 in ANCT and OSCC tissues. (g) Immunohistochemical staining score of SHMT2 in three different differentiation degrees of OSCC. (h) Western blot images and quantitative analysis of SHMT2 in NOK and OSCC cell lines. (i) Real time PCR analysis of SHMT2 in NOK and OSCC cell lines. P-values were obtained using Student's t-tests, one-way ANOVA tests, and log-rank tests. All data are shown as mean ± SD. * $p < 0.05$, ** $p < 0.01$, *** $p < 0.001$. OSCC, oral squamous cell carcinoma; ANCT, adjacent noncancerous tissue samples; NOK, normal squamous epithelial cells.

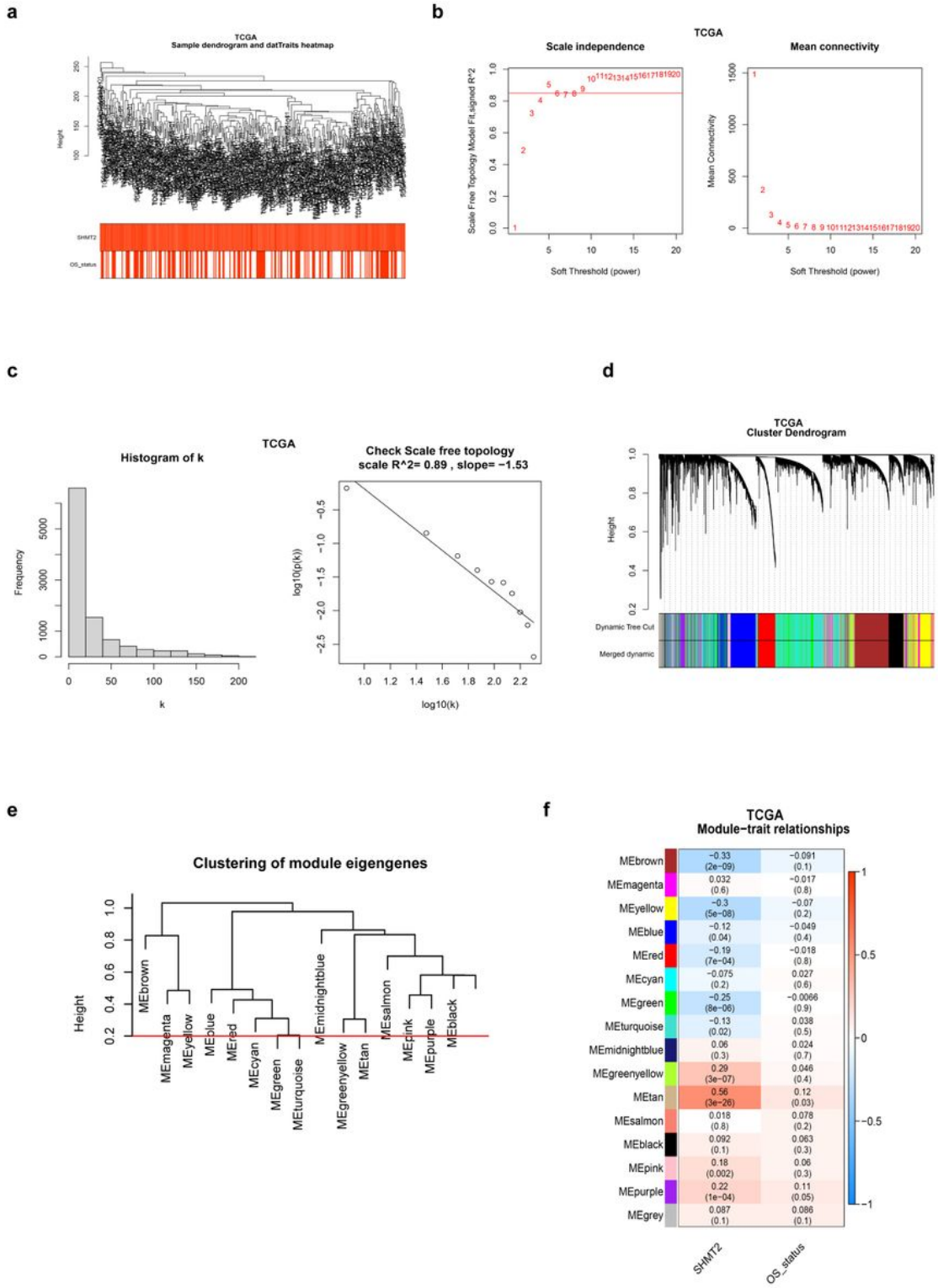


## Figure 2

Construction of weighted co-expression network and identification of the key module. (a) Hierarchical clustering dendrogram of samples in TCGA database (n = 306). (b) Analysis of the scale free fit index and the mean connectivity for various soft threshold power. (c) Scale free topology test based on  = 5. (d) Cluster dendrogram of genes with dissimilarity based on topological overlap. Branches of the clustering tree represent merged modules, and different colors correspond to different modules. (e) Cluster

dendrogram of module eigengenes: modules below the red line (0.2) are merged. (f) Correlation coefficient and p-value for module-trait relationships. Each row is a module eigengene.

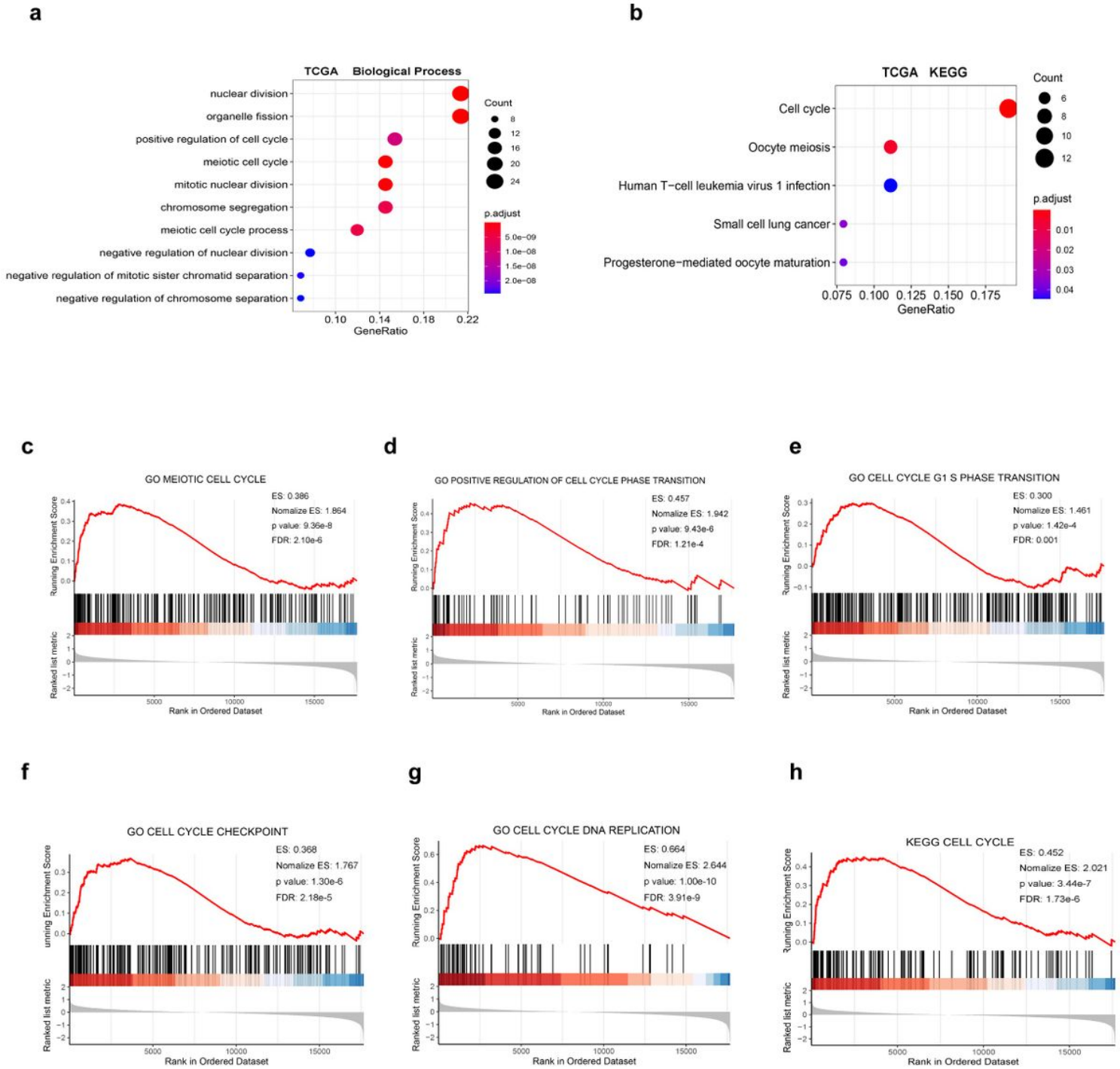


## Figure 3

SHMT2 was positively involved in cell cycle regulation of OSCC according to GO, KEGG and GSEA. (a) Biological process analysis for the key module containing SHMT2. (b) KEGG enrichment analysis for the key module containing SHMT2. (c-h) GSEA enrichment analysis: GO and KEGG pathway genes in SHMT2 high versus low samples in TCGA database. ES, enrichment score.

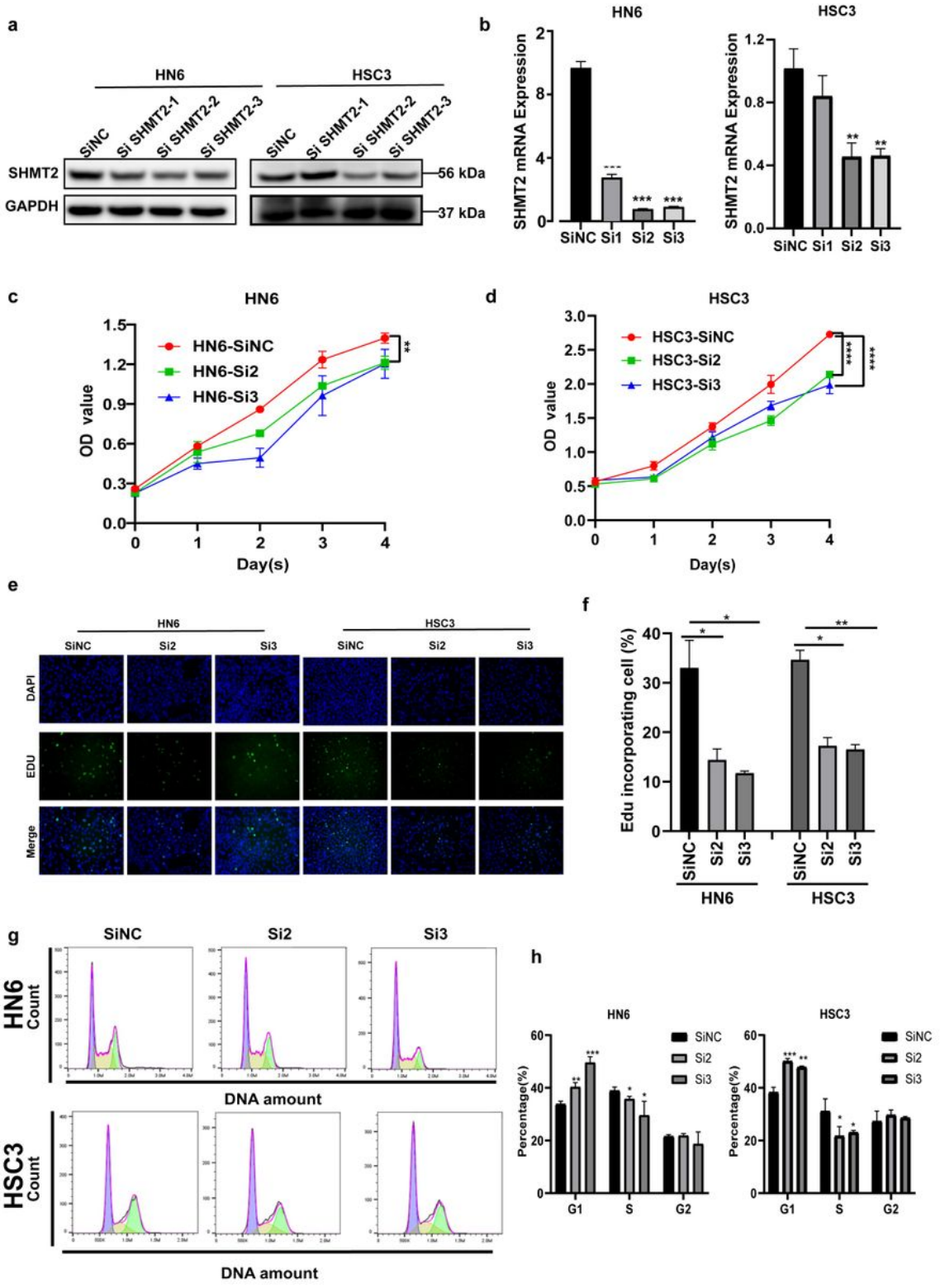


## Figure 4

Knockdown of SHMT2 inhibited the proliferation and modulates the OSCC's cell cycle in vitro. (a-b) Western blot analysis and real time PCR of HN6 and HSC3 cells transfected with SHMT2 siRNA. (c-d) CCK8 assay performed on HN6 and HSC3 cells after transfection to determine the proliferation rate. (e-f) Representative images of and quantification of Edu stained cells in negative control and SHMT2 siRNA transfected groups. (g-h) Flow cytometric analysis of indicated cells, representative graph (left) and

quantitative analysis (right). (i-j) Western blot and real time PCR analysis of several cell cycle regulators including P21, P27, CDK4, and cyclin D1 expression in indicated cells. P-values were obtained using Student's t-tests and two-way ANOVA tests * p < 0.05, ** p < 0.01, *** p < 0.001.

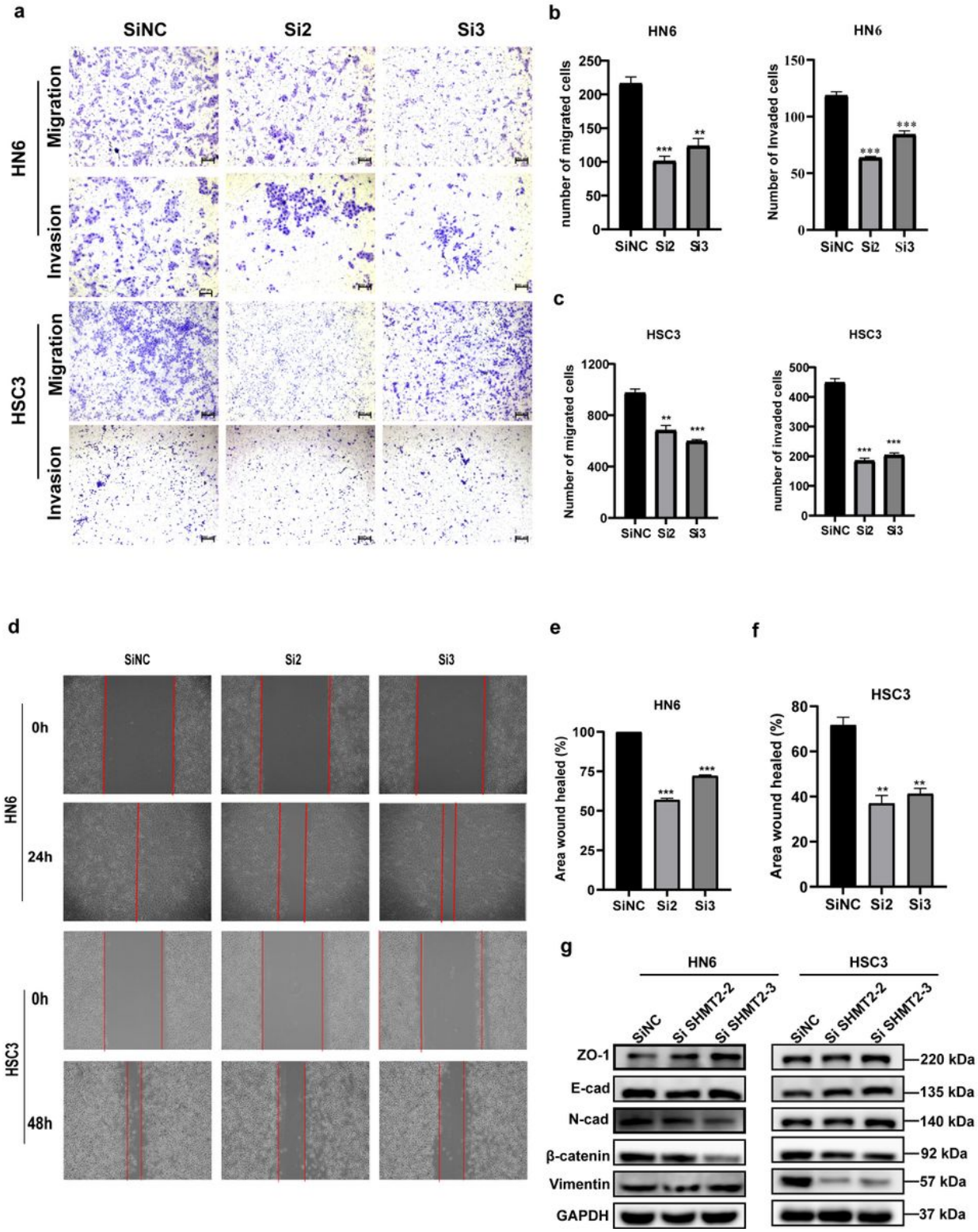


## Figure 5

Knockdown of SHMT2 impaired OSCC invasive, migrative and epithelial mesenchymal transition ability. (a) Representative photograph of transwell assays in HN6 and HSC3 cells after transfection with si-RNA

(b-c) Quantitative analysis of transwell assays in HN6 and HSC3. (d) Wound healing assay images of HN6 and HSC3 cells after SHMT2 down-regulation. (e-f) Quantitative analysis of wound healing assay in HN6 and HSC3. (g) Si-RNA treatment in HN6 and HSC3 reduced the level of ZO-1 and E-cad, while inducing the expression of N-cad, β-catenin and vimentin. P-values were obtained by Student's t-tests, * $p < 0.05$, ** $p < 0.01$, *** $p < 0.001$. E-cad, E-cadherin; N-cad, N-cadherin.

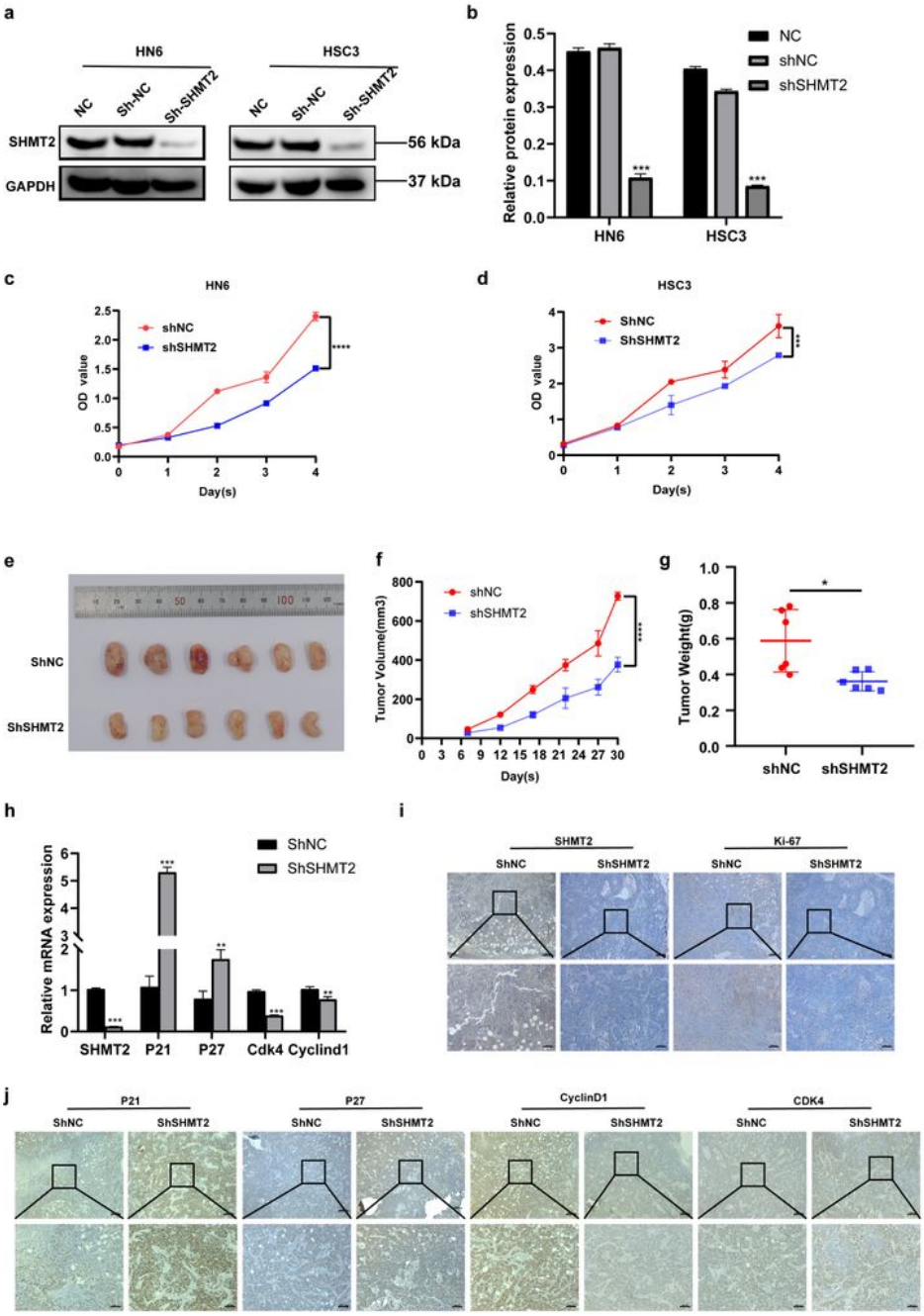


## Figure 6

Silencing SHMT2 suppressed OSCC cell growth in vivo. (a-b) Western blot analysis and quantitative calculation for cells after lentiviral transfection. (c-d) Proliferation rates for HN6 and HSC3 were detected by CCK8 assay. (e) Image for tumors taken from mice injected with shVector and shSHMT2 HN6 cells. (f) Tumor volume growth curve of mice. (g) Tumor weight was measured after mice were sacrificed. (h) Real time PCR was used to evaluate expression of SHMT2, P21, P27, CDK4, and cyclin D1 in mouse tumors. (i-j) Immunohistochemistry staining was performed to analyze protein expression of SHMT2, Ki-67, P21, P27, cyclinD1, and CDK4 in tumor tissue specimens from sh-SHTMT2 and control groups of mice. Magnification at 50× (up) and 100× (down). P-values were obtained by Student's t-tests and two-way ANOVA tests * $p < 0.05$, ** $p < 0.01$, *** $p < 0.001$. Sh, short hairpin RNA

## Supplementary Files

This is a list of supplementary files associated with this preprint. Click to download.

- Supplementarymaterial3genesoftheblackmodule.xls
- Supplementarymaterial2genesofthetanmodule.xls
- Supplementarymaterial.docx